Pergamon

Journal of Structural Geology, Vol. 17, No. 11, pp. 1507 to 1521, 1995

0191-8141/95 $9.50+0.00

0191-8141(95)00052-6

Pseudotachylyte generated in the semi-brittle and brittle regimes, Bench Canyon shear zone, central Sierra Nevada

BRENDAN A. MCNULTY

Earth Science Department, University of California, Santa Cruz, CA 95064, U.S.A.

(*Received* 21 *September* 1994; *accepted* 20 *April* 1995)

Abstract—Pseudotachylyte cuts Cretaceous plutonic and volcanic rocks in the Bench Canyon shear zone, central Sierra Nevada, California. As documented by optical and scanning electron microscopy, the pseudotachylyte displays evidence for a friction melt origin, including vesicles, amygdules, crystallites, flow fabrics and embayed crystal fragments. Based on fault-related rock association, vein morphology, and inferred crustal level of generation, two distinct types of pseudotachylyte are documented in the shear zone. Pseudotachylyte associated with cataclasite was generated at shallow crustal levels (~1–10 km) via unstable, velocity-weakening, abrasive wear friction. Pseudotachylyte associated and interlayered with mylonite was generated at deeper crustal levels (~10–15 km) most likely via stable, velocity-strengthening, adhesive wear friction; this pseudotachylyte underwent ductile deformation in the solid state. Interlayered pseudotachylyte and mylonite records cyclic aseismic/seismic slip at a transitional crustal level between the semi-brittle field of quartzofeldspathic rocks and the base of the seismogenic zone. The cyclicity is attributed to strain rate fluctuation effected by strain-resistant phacoids, pore-fluid pressure variation, ductile instabilities, or downward fault propagation.

The mode of deformation within the shear zone progressed from (i) production of mylonite during amphibolite to greenschist facies conditions, to (ii) generation of pseudotachylyte by intermittent seismic faulting within a background of aseismic shear in the upper realm of the semi-brittle field (~300–400°C), to (iii) generation of pseudotachylyte through seismic events in the brittle (<~300°C) during uplift/exhumation and cooling; some of the latter may have been generated at shallow enough crustal levels (<~4 km) to allow vesicle formation. The exhumation of a crustal level exposing such an assemblage provides a rare opportunity to study the enigmatic nature of the transitional change from semi-brittle flow to seismogenic rupturing.

INTRODUCTION

Pseudotachylyte is a fault-related rock which may occur within exhumed fault zones, and is essentially the fossil record of ancient seismic events. As such, it provides *direct* observation of the products of dynamic rupture and slip, as opposed to the indirect nature of data inferred from seismic studies. As aptly put by Shimamoto (1989), pseudotachylyte is "about the only fault rock that unequivocally indicates the past occurrence of seismogenic movement along an exhumed fault."

Generation of pseudotachylyte is a rapid dynamic process requiring sufficient displacement, velocity and slip duration in a given slip event along an active fault. The process involves many variables, including host lithology, pore-fluid pressure, confining pressure, ambient temperature, shear resistance, shear stress, slip rate/duration, and total displacement, all of which are interactive over a period of seconds (Sibson 1975; Spray 1992; Magloughlin & Spray 1992). Not surprisingly, there exists a certain mystique surrounding the subject of pseudotachylyte, partly due to the extremely dynamic, complex and poorly understood environment in which it forms, but also because of its controversial nature and the rarity of exposures worldwide.

A long-standing debate regarding pseudotachylyte is whether it is a melt product of frictional heating (Shand 1916; Philpotts 1964; Sibson 1975; Allen 1979; Maddock 1983; Spray 1987, 1992; Bossiere 1990; Killick 1990; Toyoshima 1990; Kennedy & Spray 1992; Kelley *et al.* 1994), or whether it is formed through communication or pulverization, i.e. 'ultracataclasite' (Wenk 1978; Wenk & Weiss 1982). Most workers now prefer a friction melt origin, although little agreement exists concerning the nature of the melt event. Various hypotheses include partial melts (Maddock 1986), minimum melts, (Philpotts 1964; Ermanovics *et al.* 1972), near-total melts of the non-quartz vein component (Magloughlin 1989), or melts related to melting points of individual minerals (Sibson 1975; Spray 1992, 1993). Cataclastic deformation has been shown to play a role in pseudotachylyte generation, most notably in the role of cataclastic precursors (Magloughlin 1989, 1992; Maddock 1992).

Another loosely constrained aspect of pseudotachylyte is the crustal depths at which it may be generated. The primary focus of this study is the distinction between two broad sub-classes of pseudotachylyte generated at different crustal levels during the complex long-lived deformation history of the Bench Canyon shear zone. One class of pseudotachylyte was clearly generated in the brittle regime and is associated with shear zone reactivation after significant uplift and/or exhumation. The greatest significance of this study however is the documentation of another class of pseudotachylyte marked by ductilely deformed pseudotachylyte interlayered with mylonitic rocks, an association only documented at several localities worldwide (Sibson 1980; Passchier 1982; Wenk & Weiss 1982; Hobbs *et al.* 1986; Swanson 1988). The arrays of interlayered pseudotachy-

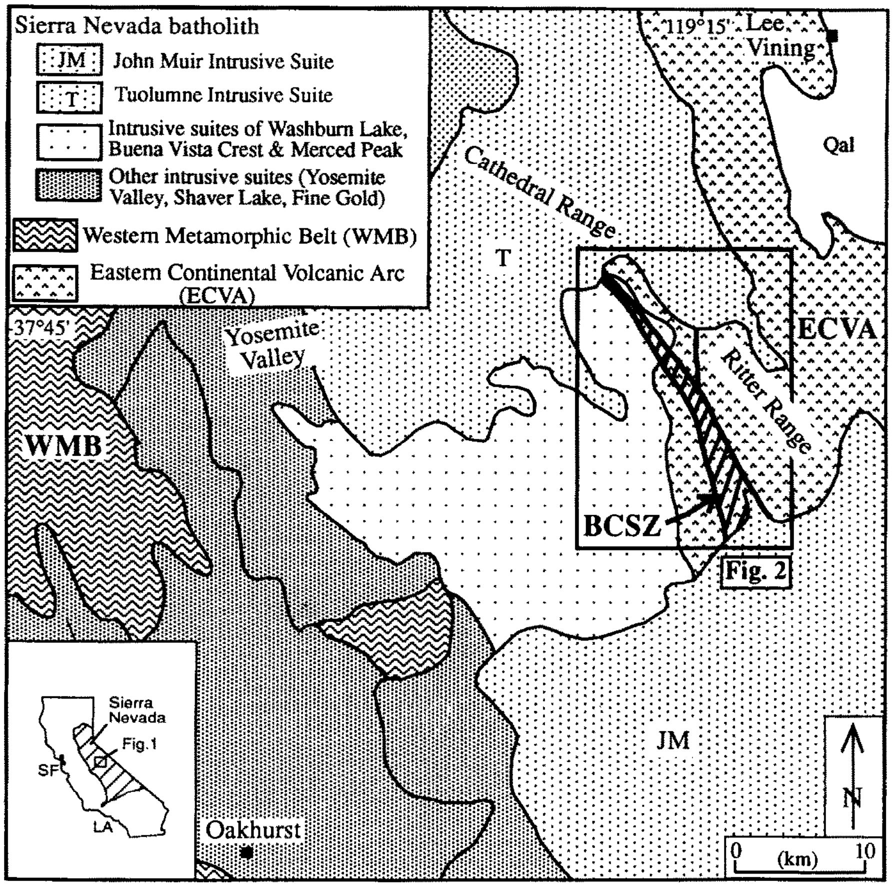

Fig. 1. Generalized geologic map showing the location of the Bench Canyon shear zone, Central Sierra Nevada, California; WMB–Western Metamorphic Belt; ECVA–eastern continental volcanic arc; inset shows location of Fig. 1; box shows Fig. 2 location. After Bateman 1992.

lyte and mylonite in the Bench Canyon shear zone portray the nature of deformation within the poorly-understood transitional region between semi-brittle flow and seismogenic rupturing. Lastly, the contrasting character of the two types of pseudotachylyte permits speculation of possible mechanical wear processes that were active during initial fault rupturing and fault slip.

GEOLOGIC SETTING

The Bench Canyon shear zone, one of the prominent Cretaceous-age shear zones in the central Sierra Nevada, California (Fig. 1), is a locus of ductile to brittle deformation containing mylonitic rock, pseudotachylyte and cataclasite (McNulty 1991, 1993, 1995). It cuts exceptionally well-exposed lower- to mid-Cretaceous volcanic rocks within the Ritter Range Pendant, and slightly younger and broadly cogenetic granitoids that intrude the volcanic section (Fig. 1). The shear zone is 20 km long and ranges in width from 0.25 to 1 km in predominantly granitic rocks to the north, to 3 km in volcanic rocks to the south (Fig. 2). As detailed in McNulty (1995) and Tobisch *et al.* (1995) and constrained through field relations, petrographic analysis, and U–Pb and $^{40}Ar/^{39}Ar$ geochronology, the deformation history of the Bench Canyon shear zone is complex and long-lived, with solid-state ductile deformation alone (i.e. mylonitic rocks) spanning a period of ~17 m.y. or longer. The long-lived, episodic and diachronous deformation history of the Bench Canyon shear zone illustrates the complexities within such zones during continental magmatic arc evolution.

Ductile deformation in the shear zone is divided into early (~101–95 Ma), main (~95–90 Ma) and late (~90–78 Ma) phases (McNulty 1991, 1995). Temperatures during main-phase deformation were between 600–300°C in a retrograde T–t path following multiple pluton emplacement between 98 and 95 Ma. Main-phase deformation involved ductile thrust movement in the 95 ± 1 Ma Red Devil Lake pluton, finger-like sills associated with the Red Devil Lake pluton, and in Cretaceous volcanic wallrocks, where thrusting was facilitated by heat and fluids associated with plutonism. Domainal and diachronous late-phase reactivation(s) along the zone involved weak, fluid-enhanced ductile deformation, and generation of abundant cataclasite and pseudotachylyte.

This study focuses primarily on pseudotachylyte in the Red Devil Lake pluton (Fig. 2). The Red Devil Lake pluton, part of the intrusive suite of Washburn Lake (Bateman 1992), has a U–Pb zircon age of 95 ± 1 Ma (Tobisch *et al.* in press), and is comprised predominantly of hornblende-biotite granodiorite. Both mylonitization and brittle deformation are best developed in the south-

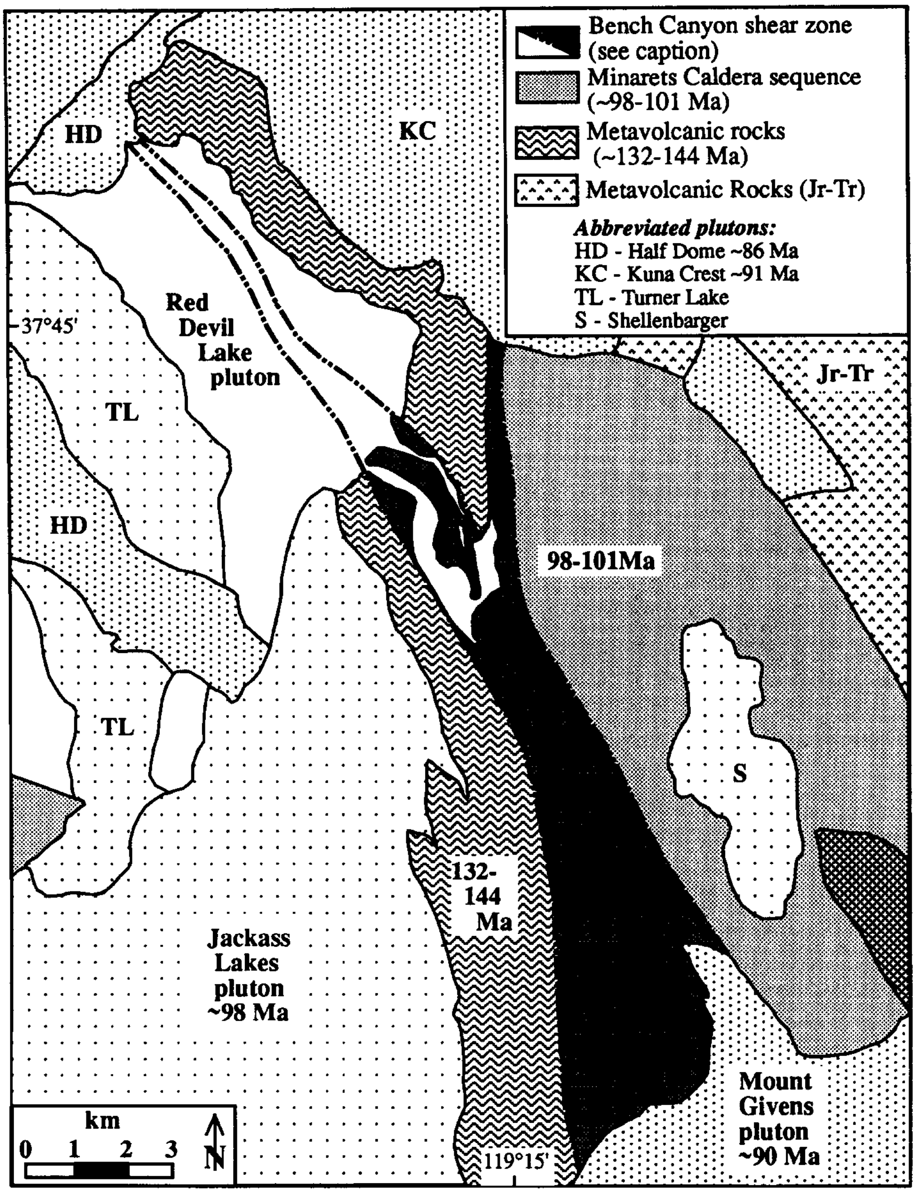

Fig. 2. Simplified geologic map shows extent of the Bench Canyon shear zone. Patterns for plutons are the same as those shown for respective intrusive suites in Fig. 1. Boundaries of the shear zone are represented by heavy dash-dot-dot lines; volcanic rocks within shear zone are shown with dark grey pattern; plutonic rocks within zone are left without this pattern for clarity. Pseudotachylyte is most prevalent in the Red Devil Lake pluton, located at the northern end of the shear zone. Modified from Peck (1980) and Huber and Rinehart (1965).

easternmost part of the pluton, and diminish in intensity to the northwest as the shear zone narrows (Fig. 2). Mylonitic foliations in the Red Devil Lake pluton generally strike northwest and dip moderately northeast, and kinematic indicators show top-to-the-southwest ductile thrust movement (McNulty 1995). It is noted that this movement sense is in marked contrast with the predominant north-east-vergent thrusting recorded elsewhere in the shear zone (McNulty 1995).

FIELD RELATIONS

Field work involved mapping and documentation of pseudotachylyte occurrence, fault-related rock associations and vein morphology. Outcrop-scale criteria consistent with that of pseudotachylyte include veins that are associated with a fault/shear zone, have sharp contacts and intrusive relations with the host rock (Figs. 3a–c), exhibit aphanitic groundmass textures (Figs. 3a–c), and contain lithic fragments derived from the host (Figs. 3a, b & d).

Two major types of pseudotachylyte occur in the Red Devil Lake pluton. The first type, designated as Pt–C, consists of pseudotachylyte intimately associated with cataclasite, occurs as broad networks of mm- to cm-scale veins, and crosscuts mylonitic rocks (Figs. 3a–d). The second type, designated as Pt–M, consists of pseudotachylyte intimately associated and interlayered with mylonite, exhibits a planar morphology, and occurs as thick bands up to 0.7 meter wide in which the pseudotachylyte may be ductilely deformed (Figs. 3e–h). The primary criteria which distinguish Pt–C from Pt–M are fault-related rock association and vein morphology.

Pt–C

Greater than 95% of the pseudotachylyte veins in the shear zone exhibit criteria diagnostic of Pt–C classification. Pt–C is characterized by: (i) association with cataclasite (Fig. 3c), (ii) irregular vein morphology (Figs. 3b & c), and (iii) cross-cutting relations with both undeformed and mylonitized granodiorite (Figs. 3a–d). The presence of cataclasite however, it *not* a prerequisite for Pt–C distinction. In contrast to the Pt–M, Pt–C is never ductilely deformed or interlayered with mylonite.

Pseudotachylyte veins present along the former rupture plane have high length-to-width ratios, extend along strike for up to tens of meters, and range in width from several millimeters to tens of centimeters (Figs. 3a–d). Plano-convex fault vein margins are present (Swanson 1988; Magloughlin 1989), and likely represent sidewall rip-outs. Injection veins branch off the fault veins obliquely (Fig. 3c), commonly intrude shear or dilatant fractures (Fig. 3b), and terminate abruptly. Fault and injection veins often form interconnected web-like networks. The varied orientations of Pt–C veins may be due to the lack of pre-existing heterogeneity, particularly in the isotropic granite, and to hydraulic fracturing driven by local melt-induced volume changes. Presumed major-slip faults are marked by thick veins encompassing large cataclastically deformed fragments (i.e. pseudotachylyte breccia of Sibson 1975, Fig. 3d). Pt–C and Pt–M pseudotachylyte are commonly obscured by late-stage cataclasis. In these cases, mylonites and pseudotachylytes are extremely disrupted, and multiple rupture events are documented by pseudotachylyte clasts within cataclasite.

Pt–M

The Pt–M pseudotachylyte makes up less than 5% of the pseudotachylyte in the shear zone. These veins (Figs. 3e–h) are associated and interlayered with mylonite and ultramylonite, for the most part exhibit planar morphology, and represent faulting localized by the strength anisotropy of the mylonitic rocks (i.e. along the foliation). Pt–M is typically ductilely deformed, containing an internal solid-state foliation and lineation (Figs. 3f–h). Solid-state foliation within the pseudotachylyte veins is defined by the plane of flattening of plastically-deformed crystal fragments, and by alignment of microcrystalline biotite. Lineations include stretching lineations defined by the long dimension of quartz crystal and lithic fragments, and mineral lineations defined by unidentifiable cryptocrystalline minerals (Fig. 4c). Lineations within the pseudotachylyte bands plunge down-dip, parallel in trend to lineations within the interlayered ultramylonite bands. Rare shear sense indicators observed within the X–Z plane of deformed pseudotachylyte bands (Fig. 3f) show top-to-the-southwest thrusting, the same as that recorded within the mylonite (McNulty 1991, 1995). However, normal sense indicators are also present. Interlayered ultramylonite and pseudotachylyte veins are locally ductilely folded into open to tight folds. Injection veins are not observed in Pt–M, and if present originally, are presumed to have been flattened.

PETROGRAPHY

Pt–C

Samples were collected and prepared for both optical and scanning electron microscopy. The pseudotachylyte groundmass consists of brown to black micro-to-cryptocrystalline material (Fig. 4a). Microcrystalline minerals that can be discerned optically include chlorite and biotite. Abundant chloritization of the groundmass possibly represents devitrification of a former glass phase (e.g. Maddock *et al.* 1987). Vein margins abruptly truncate polygonal recrystallized quartz and quartz subgrains (Fig. 4a), showing that generation of Pt–C postdates mylonitization of the host rock. Microstructures indicative of flow include a common crystallographic orientation of micro- and cryptocrystalline minerals, and the anastomosing character of this fabric around crystal fragments and into embayments along vein margins. Colour variations parallel to vein margins may represent relict flow banding. With the consideration that flow fabrics may also occur in cataclasites (Chester *et al.* 1985), they are tentatively interpreted here to be the result of migration of melt away from its generation area. Regardless, much of the pseudotachylyte lacks evidence for flow and therefore probably formed *in situ* with minimal migration.

Abundant crystal fragments and lithic clasts occur within the pseudotachylyte matrix (Fig. 4a), and exhibit the same degree of internal strain as that found in the

Fig. 3. Field photographs of pseudotachylyte veins in the Red Devil Lake pluton {pencil for scale in all except 3(d)}:(a–d) show Pt–C pseudotachylyte; (e–h) show Pt–M pseudotachylyte, (a) Pseudotachylyte veins have intrusive relations with the host rock and form sharp contacts with it; veins exhibit aphanitic groundmass and contain crystal fragments and lithic clasts derived from the host. (b) Fault veins have high length-to-width ratios and range in width from several millimeters to tens of centimeters; (c) injection veins branch off the fault veins obliquely and intrude dilatant or shear fractures. (d) Large fault zones are marked by thick veins encompassing large cataclastically-deformed fragments, forming a 'pseudotachylyte breccia'; (e) Pt–M is defined by multiple bands of pseudotachylyte interlayered with mylonite; overall thickness of this zone is 0.7 meters. (f) Close-up of 3(e) shows interlayering of Pt–M (dark-coloured layers), ultramylonite (thin light-coloured layers), and mylonite (larger sigmoidal lens-shaped bodies are present in middle of photo towards left; lenses show reverse-sense shear); the Pt–M seen here is ductilely deformed. (g) Ductilely deformed Pt–M contains internal solid-state foliation much like that in mylonitic rocks interlayered with it; (h) down-dip stretching lineations within pseudotachylyte and ultramylonite.

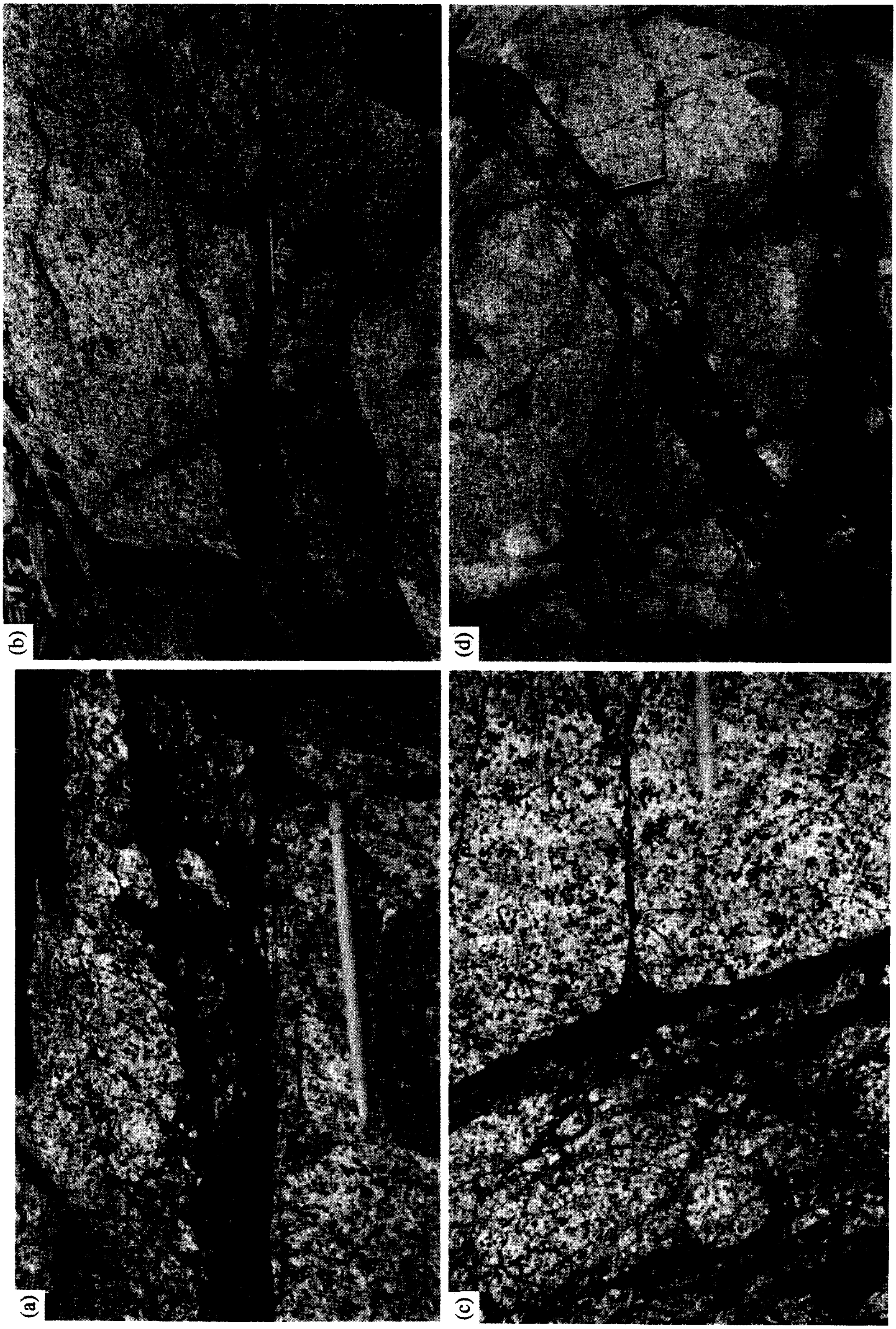

Fig. 3(a)–(d).

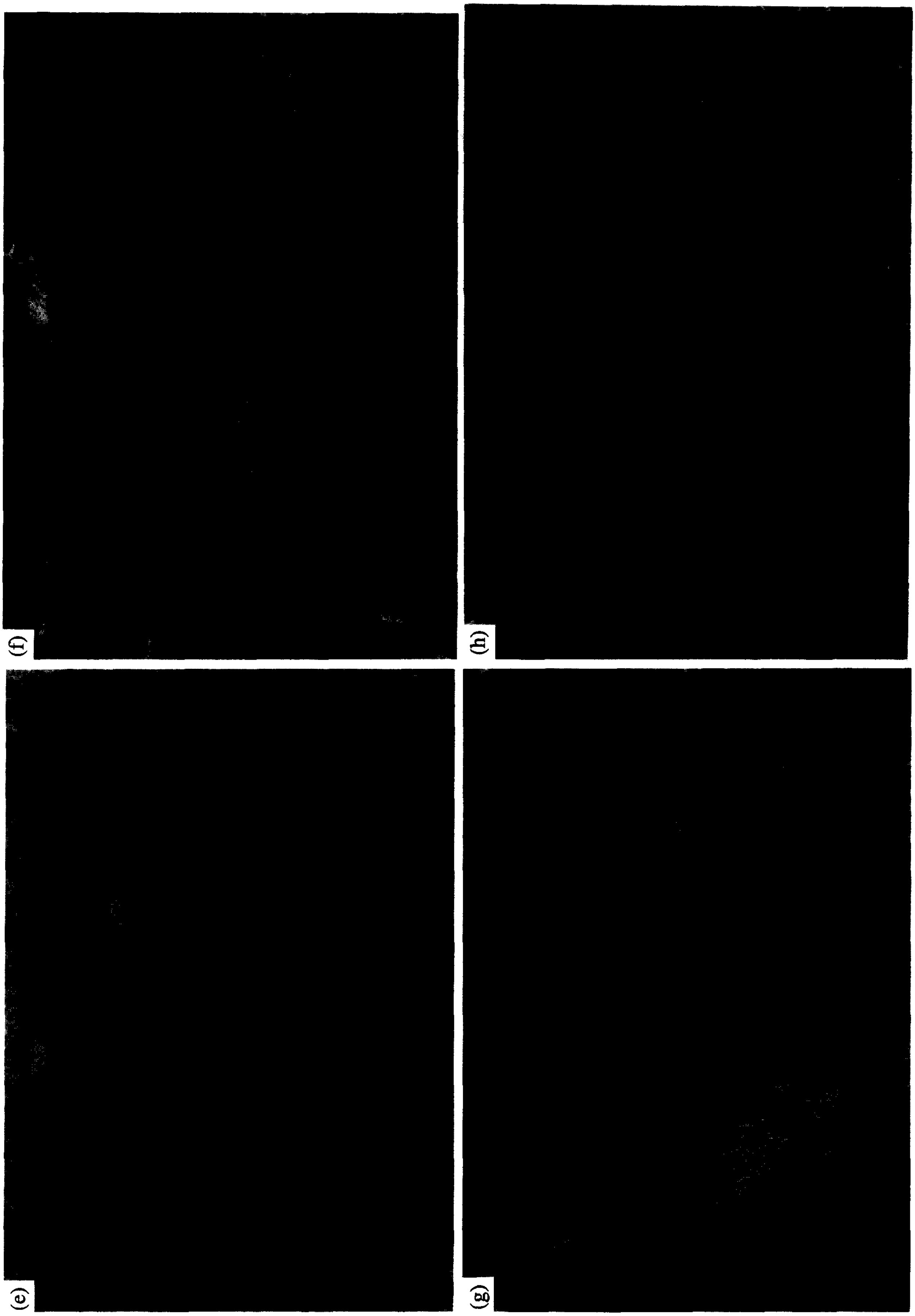

Fig. 3(e)–(h).

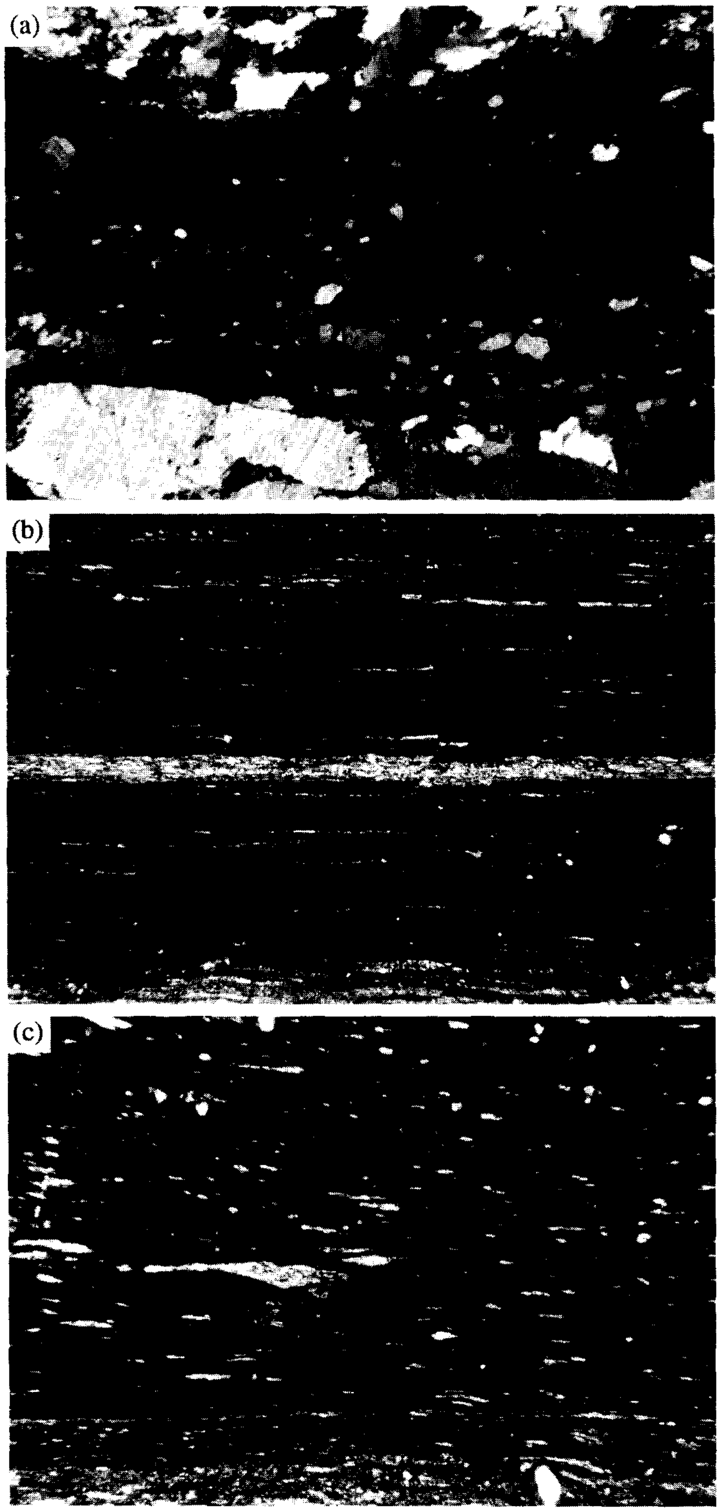

Fig. 4. Photomicrographs of pseudotachylyte. (a) Pseudotachylyte groundmass is brown to black and micro-to-cryptocrystalline; veins truncate mylonitic fabrics (e.g. recrystallized quartz). Lithic clasts and crystal fragments occur within the matrix of Pt–C veins, and exhibit the same degree of internal strain as that in the host; crystal fragments are exclusively quartz and feldspar; mica and amphibole are very uncommon. A rounded, embayed plagioclase feldspar fragment (see just below 'F') is present at the upper left corner of the vein. (b) Interlayering between pseudotachylyte and ultramylonite in Pt–M occurs on the mm-scale. (c) Crystal fragments within Pt–M are smeared out or flattened along the foliation plane, in contrast to Pt–C (Fig. 4a); crystalline fabric alignment in the matrix is observed at higher degress of magnification.

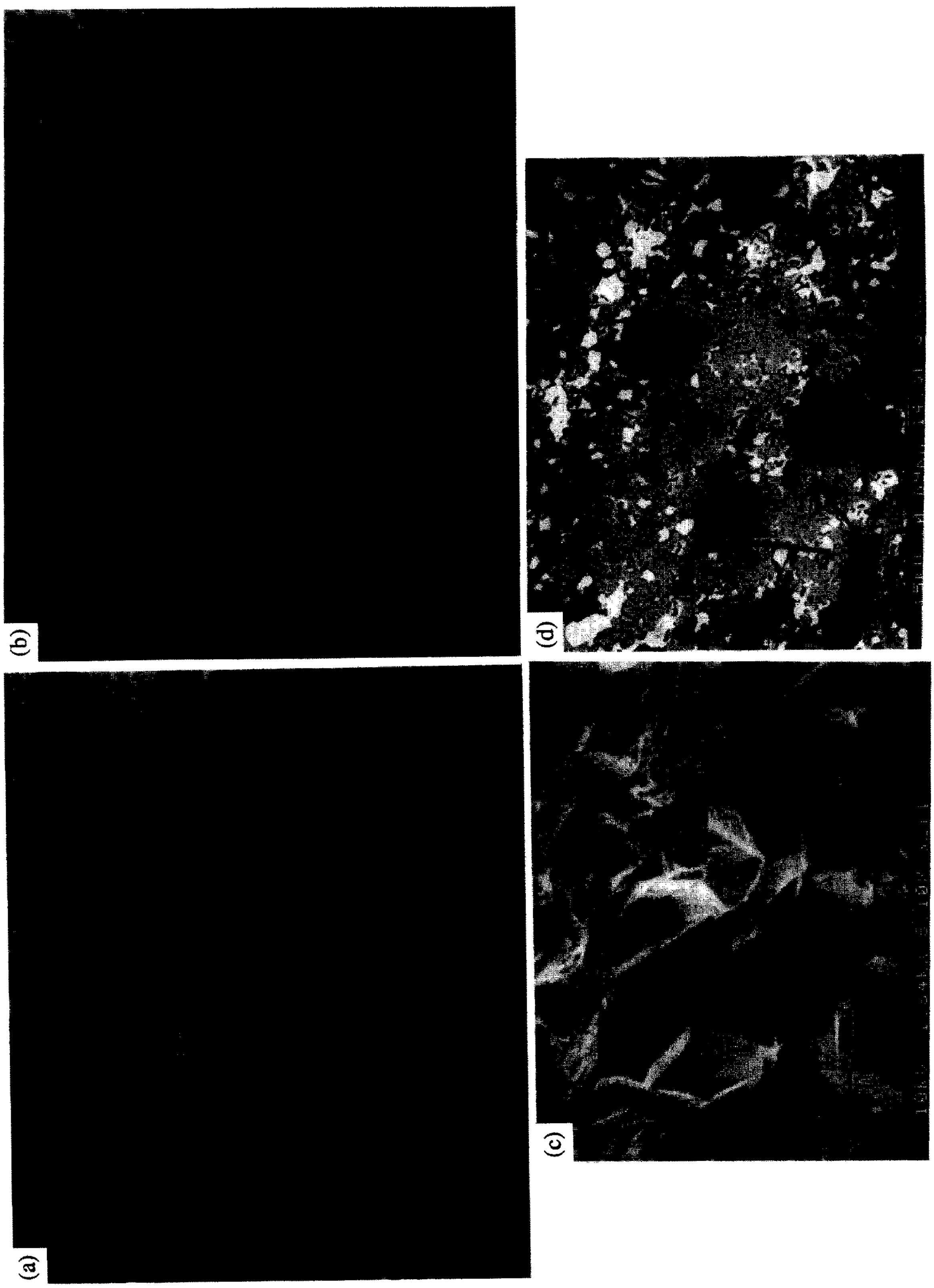

Fig. 5. SEM images; magnification intensity and scale bars (in microns) shown on bottom. (a) Micron-sized micaceous flakes (delineated by arrow) are interpreted to be crystallites quenched from a rapidly cooling melt. (b) Vesicles (delineated by arrows) present in Pt–C. (c) Micron-sized idiomorphic crystals filling the vesicle cavities are interpreted to be amygdules which crystallized from a vapor phase. (d) Back-scattered electron photomicrograph showing ubiquitous embayments (delineated by arrows) in quartz crystal fragments.

host. The crystal fragments are almost always quartz and feldspar. Mica and amphibole rarely occur as crystal fragments. Quartz fragments are angular and interpreted to be comminuted grains which have resisted assimilation. Rounding of feldspar (Fig. 4a) and occasionally quartz may be due to melt corrosion or decrepitation (Sibson 1975). Evidence of corrosion of crystal fragments, in particular ghost-like margins and diffuse interfaces, has been observed. These criteria, plus common embayments (Fig. 4a), are interpreted to be the result of assimilation of lithic clasts by a melt phase.

Pt–M

Interlayering between Pt–M and ultramylonite occurs on the mm-scale (Fig. 4b). In contrast to Pt–C, crystal fragments within Pt–M are flattened along the foliation plane (Fig. 4c), commonly with aspect ratios exceeding 20:1. The abundance of these clasts is much lower than in Pt–C. Crystal fragments within Pt–M are again predominantly quartz, and exhibit plastic deformation significantly greater than quartz porphyroclasts in the adjacent mylonite (Fig. 4c). Solid-state foliation within the pseudotachylyte is defined by the plane of flattening of the plastically-deformed crystal fragments, and by alignment of microcrystalline biotite. Insertion of a gypsum plate shows phyllosilicate alignment. While most of the Pt–M exhibits substantial ductile deformation, some of the veins contain low internal ductile strain. The presence of strain gradients within the Pt–M class indicates variable ductile overprinting.

In some domains, it is unclear whether the pseudotachylyte was generated along an earlier ultramylonitic foliation, preserving only traces of the original ultramylonite, or whether the ultramylonite was produced through ductile deformation of earlier pseudotachylyte bands (e.g. Passchier 1982). Clearly, some combination of these two options is possible, and in all likelihood, much of the ultramylonite proximal to multiple pseudotachylyte layers may be ultramylonitized pseudotachylyte.

SEM analysis

Scanning electron microscope (SEM) imaging consisted of analysis of polished, carbon-coated thin sections and mounted, platinum-coated, millimeter-sized chips of pseudotachylyte (Pt–C only). Imaging was conducted using a ISI WB–6 SEM.

Secondary electron images of the chips were instrumental in identifying the morphology of micron-scale crystals in the pseudotachylyte matrix. Micron-sized micaceous flakes are common (Fig. 5a), but their mineralogy could not be identified due to Au, Pd, and Ag X-ray spectral peaks caused by the preparatory coating. It is highly unlikely that these micaceous flakes are relict igneous minerals (i.e. crystal fragments), due to their poor chances of survival under high strain-rates typical of pseudotachylyte formation (e.g. 10^{-1} to 10^{-2} s^{-1}; Spray 1992). The flakes are interpreted to be crystallites quenched from a rapidly cooled melt.

Vesicles were also observed in SEM images (Fig. 5b). Vesicles have been documented in both naturally occurring (e.g., Maddock *et al.* 1987) and artificially generated pseudotachylyte (e.g. Kennedy and Spray 1992). Micro-sized idiomorphic crystals filling the cavities (Fig. 5c) are interpreted to be amygdules which crystallized from a vapor phase. SEM images of ubiquitous embayments in both quartz and feldspar (Fig. 5d), and of ghost-like diffuse grain boundaries, also support the presence of melt during pseudotachylyte generation.

DISCUSSION

The excellent exposure, vein morphology, and fault-related rock association of pseudotachylyte in the Bench Canyon shear zone allows a glimpse of the nature of deformation within the poorly understood transition between the semi-brittle and brittle fields of quartzofeldspathic rocks. Furthermore, the unique character of the two classes of pseudotachylyte allows assessment of fault wear mechanisms active during initial rupturing and slip. The following section briefly reviews salient characteristics of the semi-brittle regime, and of the poorly understood transition between semi-brittle and brittle regimes.

Semi-brittle field

The semi-brittle field of quartzofeldspathic rocks, also referred to as the brittle–plastic transition, lies between the plastic flow regime and the seismogenic zone. The upper limit of the plastic flow regime roughly coincides with the cessation of feldspar plasticity and the amphibolite to greenschist facies transition at $T \approx 450°C$ (Tullis & Yund 1985). Although controlled primarily by temperature, the brittle vs. plastic behavior of various minerals within the semi-brittle field is also a function of strain rate, fluid pressure, operative slip system(s), and grain size (e.g. Rutter 1976; White 1976; Paterson 1978; Tullis & Yund 1987). Brittle deformation of feldspar and amphibole within the semi-brittle field maintains an inherent pressure sensitivity of strength, and it is for this reason that early models of the "brittle-ductile transition" (e.g. Sibson 1977; Brace & Kohlstedt 1980; Kirby 1980) were oversimplified. The semi-brittle field ($450°C \geq T \geq 300°C$) is generally accepted as 10–15 km in quartzofeldspathic rocks (Fig. 6, Scholz 1988), but in the Sierra Nevada may have been substantially shallower during the mid- to late Cretaceous given the voluminous plutonism (Gettings 1988; Barton & Hanson 1989; Bateman 1992).

Within the Bench Canyon shear zone, the main phase of ductile deformation began with intrusion of the Red Devil Lake pluton at 95 ± 1 Ma, with mylonitization commencing during pluton cooling at $T \geq 600°C$ (McNulty, in press). However, the bulk of mylonitization occurred in the semi-brittle field under greenschist

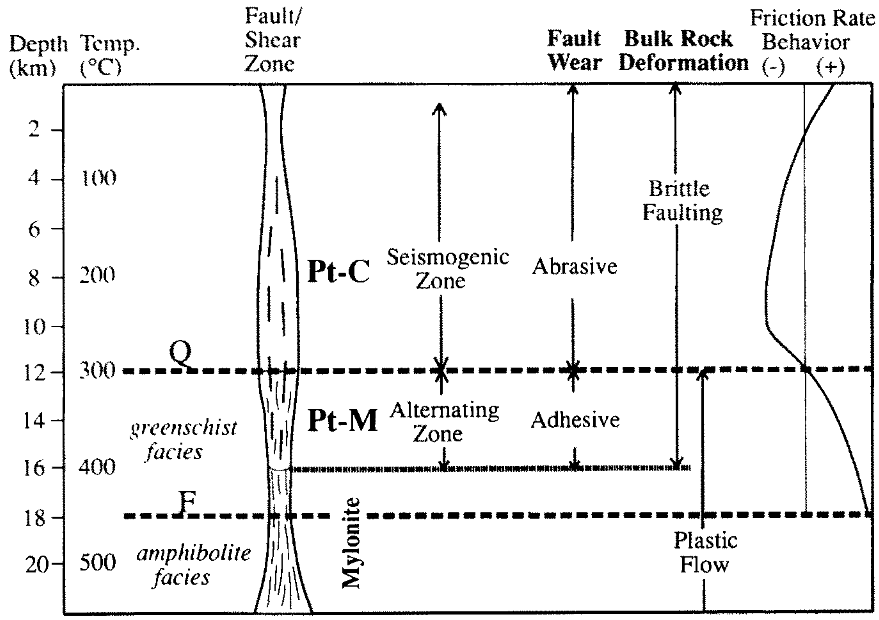

Fig. 6. The semi-brittle field of quartzofeldspathic rocks is delineated by heavy dashed lines (300–450°C) and lies between the plastic flow regime and the seismogenic zone. Rheological transitions are considered in terms of both fault wear and bulk rock deformation. Bulk rock deformation is controlled largely by mineral plasticity, i.e. quartz (Q) or feldspar (F). Mylonitization in the Bench Canyon shear zone occurred under both amphibolite and greenschist facies conditions. Pt–M formed in an 'alternating zone' at the upper realm of the semi-brittle zone that underwent cyclic aseismic/seismic slip. Pt–C formed in the seismogenic zone. Frictional sliding involved abrasive fault wear with cataclastic deformation of asperities (Pt–C), and possibly adhesive fault wear with plastic deformation of asperities (Pt–M). Friction rate behaviour evolved from velocity-strengthening (positive) to velocity-weakening (negative). Modified from Scholz (1988).

facies conditions, where quartz and biotite deformed plastically, amphibole and feldspar deformed cataclastically, and flow for the most part was ductile (Rutter 1986, Fig. 6).

Semi-brittle to brittle transition

Within the semi-brittle field, there is a gradual shift from the temperature/strain-rate dependent flow and the less pressure-sensitive crystal-plastic deformation mechanisms of the plastic regime, to the pressure-dependent linear friction and cataclastic deformation mechanisms of the seismogenic regime (Carter & Kirby 1978; Sibson 1984; Hobbs *et al.* 1986; Strehlau 1986; Rutter 1986; Scholz 1988). With decreasing confining pressure, both dilatancy and the pressure sensitivity of strength increase, result in the eventual dominance of brittle over plastic processes.

The semi-brittle to brittle transition must be considered in two contexts, one concerning the bulk deformation of rock, the other addressing the nature of frictional sliding on fault surfaces (Fig. 6). In the bulk rock, it is marked by the absence of quartz plasticity and termination of both greenschist facies metamorphism and mylonitization at $T \leq \sim 300$°C. However, the details of the shift from semi-brittle flow to brittle rupturing in the bulk rock remain poorly understood from a structural standpoint.

The nature of frictional sliding on fault surfaces is pertinent to the generation of pseudotachylyte, as it is the nature and extent of surface refinement along faults that controls whether shear heating and frictional melting occurs. Frictional sliding on fault surfaces has been considered in light of velocity-dependent friction laws, which show that frictional stress varies with the velocity of sliding and that the stability of the system is based upon velocity-strengthening vs. velocity-weakening behaviour (e.g. Scholz 1988, Fig. 8). The mechanics of this behaviour, largely understood through friction experiments on granite (Dieterich 1978; Stesky 1978; Ruina 1983; Blanpied *et al.* 1987), will be discussed later in regard to fault wear mechanisms.

Pt–M

The intimate association and interlayering of planar pseudotachylyte bands with mylonitic rocks is inferred to represent intermittent rupturing along the mylonitic foliation. The mylonitic anisotropy appears to have exerted structural control on the locus of the pseudotachylyte-generating seismic events, during which the attendant stress field must have been favorably oriented to the anisotropic weakness. An alternate possibility is that variously oriented pseudotachylyte veins were rotated into parallelism with the mylonitic foliation under the superposition of high shear strains. However, the latter is not a viable alternative where the immediate rock outside the Pt–M zones exhibits relatively low solid state strain (e.g. magmatic structures in the pluton still observable), as is the case at many localities.

The most significant aspect of Pt–M pseudotachylytes is that they underwent ductile deformation in the solid state, as indicated by solid-state foliation and lineation within the pseudotachylyte bands, and by folding of interlayered pseudotachylyte and ultramylonite. Generation of pseudotachylyte requires seismic faulting. Ductile deformation of pseudotachylyte thus implies alternating brittle/ductile deformation. The interlayered mylonite, pseudotachylyte and ductilely-deformed pseudotachylyte in the Bench Canyon shear zone are therefore interpreted to record cyclic aseismic/seismic slip in the upper realm of the semi-brittle field, i.e., proximal to the transition between semi-brittle flow and seismogenic rupturing.

Possible mechanisms/processes for generation of Pt–M

First, the possibility that pseudotachylyte was ductilely deformed as a function of younger, intrusion-driven geotherm inflation must be addressed. In the immediate area, the only plutonism younger than the Red Devil Lake pluton involved emplacement of the Tuolumne Intrusive Series from ~91 to ~83 Ma (Stern *et al.* 1981; Bateman 1992; Fleck & Kistler 1994, fig. 1). None of these plutons have aureoles that extend to the area containing the ductilely deformed pseudotachylyte. The latter only occurs within the south-easternmost margin of the Red Devil Lake pluton, a distance of at least seven kilometers away from the marginal megacrystic facies of the Half Dome pluton (~86 Ma; Fleck & Kistler 1994), and three kilometers from the Kuna Crest pluton (Fig. 2). It is highly unlikely that temperatures within the aureoles of those plutons exceeded 300°C at that distance. Furthermore, ^{40}Ar–^{39}Ar geochronology conducted on igneous biotite outside the shear zone and metamorphic biotite within the shear zone yielded ages of 86 ± 0.2 Ma and 84.9 ± 0.2 Ma, respectively (Fig. 7, Tobisch *et al.* 1995, McNulty 1995). Thus, the Red Devil Lake pluton probably did not cool through 300 ± 50°C (Harrison *et al.* 1985, and ref. within) until ~86–85 Ma, later than intrusion of either the Half Dome or Kuna Crest plutons. Intrusion-driven geotherm inflation is thus discounted as a mechanism for ductile deformation of pseudotachylyte.

Possible processes that may have produced the seismic/aseismic cyclicity are discussed below, and are all variants based upon a unifying theme of strain-rate fluctuation.

(1) Frictional melting along a fault surface involves the complex coupled interaction of thermal, fluid pressure and stress fields (Sibson 1975; Mase & Smith 1985, 1987). The role of water may play an important part in pseudotachylyte generation. For example, thermal pressurization along a fault ceases a decrease in effective stress, cohesion and dynamic shear strength, thereby prohibiting the temperatures required for frictional heating. Conversely, Mase & Smith (1985) showed that, given permeability and compressibility of the porous medium in excess of 10^{-15} m^2 or 10^{-8} Pa^{-1}, thermal expansion of pore fluids does not reduce the dynamic shear strength of a fault. Frictional heating and formation of pseudotachylyte, which requires high shear stress seismic events, would thus be possible. If variations in hydraulic parameters occurred at a time when T ≈300°C in the Bench Canyon shear zone (i.e. at the semi-brittle to brittle transition), it is possible that episodic seismic and aseismic slip, respectively, could be a function of 'drained' vs. 'undrained' conditions in the zone.

(2) Uplift and/or exhumation of the shear zone, or strain hardening within it, may have facilitated its passage out of the semi-brittle field into the lowermost region of the brittle field, within which seismic generation of Pt–M occurred. In this spatially restricted zone, ductile strain could still be partitioned to the fine-grained and inherently weaker pseudotachylyte bands, and would occur at lower differential stresses than would be necessary for further brittle failure (Passchier 1982, Stel 1986).

(3) Downward propagation of seismogenic ruptures into the predominantly aseismic regime may account for generation of 'deep-level' pseudotachylyte (Sibson 1977, Das 1982, Tse & Rice 1986, Strehlau 1986, Scholz 1988). Large earthquakes which nucleate in the vicinity of the deepest regions of the brittle regime may propagate down to the strength maxima in the semi-brittle field (Fig. 6), and induce strain rates many orders of magnitude greater than prevailing tectonic strain rates. Stress relaxation which follows seismic strain rates then facilitates ductile deformation of pseudotachylyte at aseismic strain rates. Deep intraplate earthquakes which have been documented (e.g. in the 6.9 km/s crustal layer), tend to occur within 'cold' regions with low heat flow (Wong & Chapman 1990). An example exists in the western Sierra Nevada, where micro-earthquake monitoring showed modern seismicity to be confined to depths of 12 to 38 km (Wong & Savage 1983). Although these studies of modern seismicity show that earthquakes may occur at deep crustal levels under cold conditions (i.e. T ≤ 300°C), the brittle–plastic transition in the Sierra Nevada during the Cretaceous must have been substantially elevated by plutonism (cf. Gettings 1988). If applicable to the ductilely deformed pseudotachylyte in the Bench Canyon shear zone, the process of downward seismogenic rupturing would therefore have occurred at a relatively high crustal level.

(4) Fluctuating strain rates may be induced by strain-resistant phacoids within the semi-brittle field (e.g. 'stress risers' of Sibson 1980). Several meter-scale lens-shaped pods of low-strain granodiorite in the Red Devil Lake pluton are bounded by high-strain mylonite/pseudotachylyte zones, and it is conceivable that heterogeneous strain build-up around these pods may have produced intermittent seismic events within a background of semi-brittle flow. In this manner, pseudotachylyte may form at the same crustal level as mylonitic rocks.

(5) Hobbs *et al.* (1986) proposed that unstable ductile shearing, i.e. ductile instabilities, could produce pseudotachylyte in rocks otherwise undergoing ductile deformation in the semi-brittle field. These ductile instabilities are attributed to both stress relaxation associated with thermal fluctuations, which must exceed work hardening associated with strain rate fluctuation, and to stored elastic strain energy in the surrounding rock.

(6) The experimental halite shear zone model of

Shimamoto (1989) shows that both S–C mylonitization and brittle faulting occur in a 'semi-ductile' regime, a zone he defined as that in which microstructural textures are virtually indistinguishable from those developed in the 'fully ductile' (i.e. plastic flow) regime. Significantly, Shimamoto showed that strength in this regime is *pressure, slip rate, and temperature* dependent. S–C mylonites therefore represent some component of *frictional behaviour*, as opposed to bulk shearing; C-surfaces in particular may undergo slip and adhesive-wear friction (Scholz 1988, Shimamoto 1989). In this manner, strain localization and high slip rates may lead to formation of pseudotachylyte. A corollary derived from Shimamoto's work is that S–C mylonites in the Bench Canyon shear zone may have formed at seismogenic depths, precluding the need for downward propagation of earthquakes into the 'fully ductile' regime. The model also shows that stick-slip events in this 'semi-ductile' regime are accompanied by aseismic slip before *and after* the seismic event, which may also explain the ductile deformation of pseudotachylyte. Lastly, the model is monocrystalline, implying that even more complex flow regime transitions in polycrystalline rocks are likely.

All of the above parameters, in addition to fault wear mechanisms discussed below, may be incorporated into the fault/shear zone model proposed by Scholz (1988, fig. 6). Scholz invoked an 'alternating zone' between the semi-brittle field and the seismogenic zone that may undergo alternating semi-brittle flow and coseismic slip. Episodic/seismic slip within the 'alternating zone' may occur under a temperature range of 300–400°C. Within this model, coeval and/or cyclic generation of pseudotachylyte and mylonite would be expected.

It is clear that cyclic seismic/aseismic shear occurred at the same crustal level in the Bench Canyon shear zone, i.e. seismic events penecontemporaneous with ductile thrusting. Periodic strain rate fluctuation is ultimately responsible for the generation of Pt–M pseudotachylyte at relatively deep crustal levels. The possible scenarios for initiating strain rate fluctuation are less well constrained, as generation of Pt–M may be facilitated by any or all of the six parameters listed above. More rigorous fault/shear zone modelling is needed for the transitional zone between the upper realm of the semi-brittle field and the base of the seismogenic zone. One of the key questions regarding this zone is how much strain the bulk rock undergoes, versus how much is taken up along faults through frictional sliding (Scholz 1988).

Pt–C

Pseudotachylyte associated with cataclasite, and the cross-cutting relation between pseudotachylyte and mylonite, indicate generation of Pt–C in the brittle field of quartzofeldspathic rocks (i.e. upper 10 km, Fig. 6, Sibson 1977, Swanson 1992). Furthermore, the occurrence of vesicles and amygdules in pseudotachylyte implies low lithostatic pressure conditions and generation most likely in the upper 4 km of the crust (Maddock *et al.* 1987, Magloughlin 1992). Crystallized pseudotachylyte melt ('microlitic pseudotachylyte') may require crustal depths of 4–5 km (Sibson 1975, 1977, Allen 1979, Swanson 1992), although it has been noted that the presence or absence of microlites may also reflect host/melt compositional variables and/or the kinetics of crystal nucleation (Maddock 1986).

Retrograde metamorphic reactions, microstructures and ^{40}Ar–^{39}Ar geochronology generally show decreasing temperatures in the Bench Canyon shear zone during mylonitization (McNulty 1995, Fig. 7, Tobisch *et al.* 1995). As discussed previously, ^{40}Ar–^{39}Ar ages indicate that the Red Devil Lake pluton probably did not cool through 300 ± 50°C until ~86–85 Ma. Thermobarometric and thermochronologic data from the ~90 Ma Mount Givens pluton shows rapid post-90 Ma cooling (i.e. >160°C/m.y., Renne *et al.* 1993). These data and other biotite dates from the region (e.g. Tobisch *et al.* 1995) suggest that much of the regional uplift/exhumation and concomitant cooling of the region occurred from ~90 to ~85 Ma. Petrographic studies (e.g. Mansfield 1979) indicate dramatic increases in arc-derived sediment in Great Valley sequences from ~97 Ma to ~83 Ma, supporting pluton unroofing and significant exhumation of the central Sierra Nevada during this time. Generation of Pt–C, which required ambient temperatures less than 300°C, is then inferred to have occurred post-85 Ma after significant uplift and/or exhumation of the region. Ongoing deformation involved further cataclastic formation, and infiltration of water as demonstrated by epidote-bearing veins cutting pseudotachylyte. The abundance of fluids late in the history may have prevented further pseudotachylyte formation.

Fault-wear Models

The contrasting character of the two types of pseudotachylyte allows speculation on the nature of mechanical wear processes active during initial rupturing and fault slip. Initial earthquake rupture is followed by the linkage of fracture arrays and subsequent decoupling, which at the grain scale may be facilitated by either plastic (adhesive) or cataclastic (abrasive) wear mechanisms (Figs. 6 and 8). Pt–M may be explained by an adhesive-wear friction fault model; Pt–C by an abrasive-wear friction fault model.

Adhesive wear: Pt–M

It is useful to first think of the transition between semi-brittle flow and seismogenic faulting in terms of frictional sliding, keeping in mind that frictional behaviour is not restricted to brittle faulting (e.g. Scholz 1988). Increasing confining pressure with depth increases frictional resistance and causes a linear increase in differential stress at failure, accompanied by a smaller stress drop to some value of residual frictional strength; the brittle–plastic transition, or semi-brittle field, occurs where frictional resistance equals the rock's shear strength (Sibson 1977). It is within the deepest crustal levels within which deformation is still frictional, i.e.

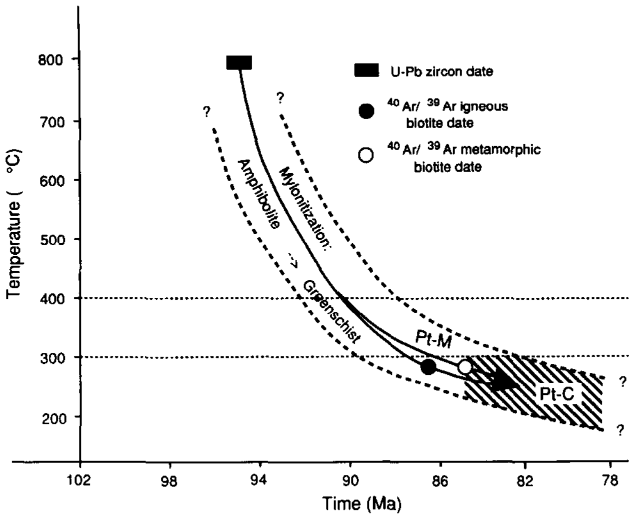

Fig. 7. Schematic time–temperature graph for the Red Devil Lake pluton showing U–Pb zircon and ^{40}Ar–^{39}Ar geochronology (Tobisch *et al.* 1995, McNulty 1995). Closure temperatures are: zircon: >800°C (Heamon & Parrish 1991); biotite: 300 ± 50°C (Harrison *et al.* 1985, and references within). The approximate timing of mylonitization and Pt–M/Pt–C pseudotachylyte generation are inferred.

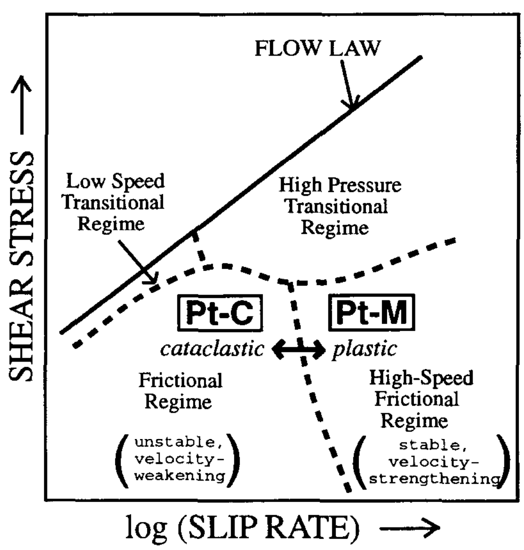

Fig. 8. Possible model showing the velocity dependence of shear resistance. The high-speed frictional regime is marked by a positive correlation between friction and slip rate; the frictional regime is marked by a negative correlation between friction and slip rate (see text). The friction–velocity relationships delineated by a synthetic shear zone model (Shimamoto 1989), and by friction experiments on granite, explain the generation of the Pt–C and Pt–M series pseudotachylytes in the Bench Canyon shear zone. Wear of asperities is shown as either cataclastic or plastic. Modified from Shimamoto (1989).

strength increases with confining pressure, that Pt–M is interpreted to have been generated (Fig. 6).

An adhesive wear-dominant fault model explains many features of Pt–M, including:

(1) highly strained (i.e. 20:1 aspect ratio) quartz crystals in the pseudotachylyte matrix (Fig. 4c);
(2) lower frequency of these clasts relative to Pt–C (Fig. 3f);
(3) planar morphology of the veins (Figs 3e–g);
(4) significantly greater composite vein thickness (Fig. 3e);
(5) ubiquitous association and intimate interlayering of pseudotachylyte and mylonite (Figs. 3e–h).

Friction along a fault zone during adhesive wear is stable and velocity-strengthening, i.e. friction increases with increasing slip velocity (Rabinowicz 1965; Shimamoto 1986; Swanson 1992). This zone is shown in Fig. 8 as the high-speed frictional regime. This type of behaviour also occurs in fault gouge (Fig. 6). Ruptures occur as reactivations along the mylonitic anistropy (Figs. 3f & g), promoting planar layer-parallel slip, minimal asperity formation and low wear rates. Rapid surface refinement along the fault allows the area of contact between opposing slip surfaces to approach the total area, leading to total adhesion. This promotes *plastic deformation* of asperities and smearing of material to opposite slip surfaces, which may increase the likelihood of frictional heating and therefore pseudotachylyte generation (Swanson 1992). With plastic deformation of asperities, there is little initial abrasive wear and therefore no cushion of cataclasite. Pseudotachylyte veins will more likely be planar (repeated events along same anisotropy), thicker, and relatively devoid of crystal fragments and lithic clasts, features all common to Pt–M in the Red Devil Lake pluton (Figs. 3e–h). Continued aseismic movement may then result in pervasive ductile deformation of the pseudotachylyte (Fig. 4c).

Abrasive wear: *Pt–C*

An abrasive wear-dominant fault model explains features of Pt–C, including:

(1) great abundance of quartz crystals and lithic clasts in the matrix;
(2) angular shape and low internal strain of these fragments;
(3) varied morphology of the veins;
(4) association with cataclastic fault-related rocks (Figs. 3a–d, and 4a).

During abrasive wear, unstable velocity-weakening friction occurs under low temperature and confining pressure (Figs. 6 and 8, Rabinowicz 1965, Shimamoto 1986, Swanson 1992). Velocity-weakening behaviour involves a negative correlation between velocity and friction, i.e. as friction increases, velocity decreases and stick-slip behavior dominates. Initial cataclastic deformation leads to *fracturing* of asperities; fault-related rocks are mostly cataclasite and ultracataclasite; pseudotachylyte forms where slip rates are high enough to melt some of the aggregate through frictional heating (Spray 1987, 1992).

CONCLUSIONS

As shear zones evolve, slip may result in development of both seismic and aseismic structures. The Bench Canyon shear zone in the central Sierra Nevada, California, underwent a complex episodic deformation history and was probably active through much of its uplift/exhumation. The mode of deformation within the shear/fault zone progressed from (i) aseismic shearing which produced mylonites during amphibolite to greenschist facies conditions, to (ii) generation of Pt–M through intermittent seismic faulting within a background of aseismic shear in the upper realm of the semi-brittle field (300–400°C), i.e., seismic events penecontemporaneous with ductile thrusting, to (iii) generation of Pt–C through repeated seismic events in the brittle regime (<~300°C) during uplift/exhumation and cooling; some of the latter may have been generated at shallow enough crustal levels to allow vesicle formation. The occurrence of a friction melt event during seismic faulting is suggested by optical and SEM evidence for vesicles, amygdules, sub-rounded cataclastic fragments, embayed crystal fragments, flow fabrics, and what appears to be crystallites.

The character of the different types of pseudotachylyte in the shear zone may be explained through the nature of mechanical processes active during initial rupturing and fault slip. Although both types are attributed to frictional melting, Pt–C may be explained by an abrasive wear-dominant fault model (unstable, velocity-weakening friction); Pt–M by an adhesive wear-dominant fault model (stable, velocity-strengthening friction). The key difference in the friction wear models is that initial rupturing and slip was facilitated by fracturing of asperities in Pt–C, as opposed to initial plastic deformation of asperities in Pt–M. Plastic deformation of asperities in Pt–M may have increased the likelihood of frictional heating and therefore pseudotachylyte generation. More work, possibly using analog models, needs to be conducted to better understand the mechanics and by-products of friction wear.

This study confirms that intermittent aseismic/seismic slip may occur at a given crustal level within a shear zone. Many variables are associated with generation of deep-level pseudotachylyte, and it is clear that the transition between semi-brittle flow and seismic faulting cannot be delineated by a simple boundary in P–T strain-rate fluid deformation mechanism space. Instead, the nature of deformation within this transient zone may be extremely variable in space and time and dependent on many parameters. The exhumation of a crustal level exposing such an assemblage of fault-related rock in the Bench Canyon shear zone allows a rare glimpse of the enigmatic transitional zone between plastic and brittle deformation.

Acknowledgements—This work was made possible by grants from NSF (EAR-9002672 and EAR-9204712 awarded to Othmar Tobisch), the Geological Society of America and Sigma Xi. I thank O. Tobisch for encouraging me to pursue my interest in pseudotachylyte, J. Krupp for guidance with SEM and photographic procedures, and J. Magloughlin, L. Goodwin and J. Evans for reviews.

REFERENCES

Allen, A. R. 1979. Mechanism of frictional fusion in fault zones. *J. Struc. Geol.* **1**, 231–243.

Barton, M. D. & Hanson, R. B. 1989. Magmatism and the development of low-pressure metamorphic belts: implications from the western United States and thermal modeling. *Geol. Soc. Am. Bull.* **100**, 1051–1065.

Bateman, P. C. 1992. *Plutonism in the central part of the Sierra Nevada batholith, California*, U.S. Geol. Surv. Prof. Pap. 1483, 186.

Blanpied, M. L., Tullis, T. E. & Weeks, J. D. 1987. Frictional behavior of granite at low and high sliding velocities. *Geophys. Res. Lett.* **14**, 554–557.

Bossiere, G. 1991. Petrology of pseudotachylites from the Alpine fault of New Zealand. *Tectonophys.* **186**, 173–193.

Brace, W. F. & Kohlstedt, D. L. 1980. Limits on lithospheric stress imposed by laboratory experiments. *J. Geophys. Res.* **85**, 6248–6252.

Carter, N. L. & Kirby, S. H. 1978. Transient creep and semibrittle behavior of crystalline rocks. *Pure Appl. Geophys.* **116**, 807–839.

Chester, F. M., Friedman, M. & Logan, J. M. 1985. Foliated cataclasites. *Tectonophys.* **111**, 139–146.

Das, S. 1982. Appropriate boundary conditions for modeling very long earthquakes and physical conditions. *Bull. Seismol. Soc. Am.* **72**, 1911–1926.

Dieterich, J. H. 1978. Time-dependent friction and the mechanics of stick-slip. *Pure Appl. Geophys.* **116**, 790–806.

Ermanovics, I. F., Helmstaedt, H. & Plant, A. G. 1972. An occurrence of Archean pseudotachylite from southeastern Manitoba. *Can. J. Earth Sci.* **9**, 257–265.

Gettings, M. E. 1988. Variation of depth to the brittle–ductile transition due to cooling of a midcrustal intrusion. *Geophys. Res. Lett.* **15**, 213–216.

Harrison, T. M., Duncan, I. & McDougall, I. 1985. Diffusion of ^{40}Ar in biotite: temperature, pressure and composition effects. *Geochim. Cosmochim. Acta*, **49**, 2461–2468.

Heamon, L. & Parrish, R. 1991. U–Pb geochronology of accessory minerals. In: *Short Course Handbook on Application of Radiogenic Isotope Systems to Problems in Geology*, Vol. 19, *Mineralogical Society of Canada, Toronto* (edited by Heamon, L. & Ludden, T. N.). 59–102.

Hobbs, B. E., Ord, A. & Teyssier, C. 1986. Earthquakes in the ductile regime? *Pure App. Geophys.* **142**, 309–336.

Kelley, S. P., Reddy, S. M., & Maddock, R. 1994. Laser-probe ^{40}Ar/^{39}Ar investigation of a pseudotachylyte and its host rock from the Outer Isles thrust, Scotland. *Geology*, **22**, 443–446.

Kennedy, L. A. & Spray, J. G. 1992. Frictional melting of sedimentary rock during high-speed diamond drilling: an analytical SEM and TEM investigation. In: *Frictional Melting Processes and Products in Geological Materials, Tectonophys.* (edited by Magloughlin, J. F. & Spray, J. G.). **204**, 323–337.

Killick, A. M. 1990. Pseudotachylite generated as a result of a drilling burn-in. *Tectonophys.* **171**, 221–227.

Kirby, S. H. 1980. Tectonic stress in the lithosphere; constraints provided by the experimental deformation of rocks. *J. Geophys. Res.* **85**, 6353–6363.

Maddock, R. H. 1983. Melt origin of fault generated pseudotachylites as demonstrated by textures. *Geology*, **11**, 105–108.

Maddock, R. H. 1986. Partial melting of lithic porphyroclasts in fault-generated pseudotachylites. *Neues. Jb Miner. Abh.* **155**, 1–14.

Maddock, R. H., Grocutt, J., and van Ness, M. 1987. Vesicles, amygdales, and similar structures in fault-generated pseudotachylites. *Lithos*, **20**, 419–432.

Maddock, R. H. 1992. Effects of lithology, cataclasis and melting on the composition of fault-generated pseudotachylytes in Lewisian gneiss, Scotland. In: *Frictional Melting Processes and Products in Geological Materials, Tectonophys.* (edited by Magloughlin, J. F. & Spray, J. G.). **204**, 261–278.

Magloughlin, J. F. 1989. The nature and significance of pseudotachylite from the Nason terrane, North Cascades Mountains, Washington. *J. Struct. geol.* **11**, 907–917.

Magloughlin, J. F. 1992. Microstructural and chemical changes associated with cataclasis and friction melting at shallow crustal levels: the cataclasite-pseudotachylyte connection. In: *Frictional Melting Processes and Products in Geological Materials. Tectonophys.* (edited by Magloughlin, J. F. & Spray, J. G.). **204**, 243–260.

Magloughlin, J. F. & Spray, J. G. 1992. Frictional melting processes and products in geological materials: introduction and discussion. In: *Frictional Melting Processes and Products in Geological Materials, Tectonophys.* (edited by Magloughlin, J. F. & Spray, J. G.). **204**, 197–206.

Mansfield, C. F. 1979. Upper Mesozoic subsea fan deposits in the southern Diablo Range, California: Record of the Sierra Nevada magmatic arc. *Geol. Soc. Am. Bull.* **90**, 1025–1046.

Mase, C. W. & Smith, L. 1985. Pore fluid pressures and frictional heating on a fault surface. *Pure App. Geophys.* **122**, 583–607.

Mase, C. W. & Smith, L. 1987. Effects of frictional heating on the thermal, hydrologic, and mechanical response of a fault. *J. Geophys. Res.* **92**, 6249–6272.

McNulty, B. A. 1991. Development of mylonite and pseudotachylite in the Bench Canyon shear zone, Central Sierra Nevada, California. *Geol. Soc. Am. Abs. w/Prog.* **23**, 176–177.

McNulty, B. A. 1993. Pseudotachylyte in the Bench Canyon shear zone, central Sierra Nevada, California: frictional melting in the brittle and semi-brittle fields. *Geol. Soc. Am. Abs. w/Prog.* **25**, 119.

McNulty, B. A. 1995. Shear zone development during magmatic arc construction: the Bench Canyon shear zone, Central Sierra Nevada, California. *Bull. Geol. Soc. Am.*

Passchier, C. W. 1982. Pseudotachylite and the development of ultramylonite bands in the Saint Barthelemy Massif, French Pyrenees. *J. Struct. Geol*, **4**, 69–79.

Paterson, M. S. 1978. *Experimental Rock Deformation–the Brittle Field.* Springer-Verlag, 254.

Philpotts, A. R. 1964. Origin of pseudotachylites. *Am. J. Sci.* **262**, 1008–1035.

Rabinowicz, E. 1965. *Friction and Wear of Materials.* John Wiley and Sons, New York, 243.

Renne, P. R., Tobisch, O. T. & Saleeby, J. B. 1993. Thermochronologic record of pluton emplacement, deformation and exhumation at Courtright shear zone, Central Sierra Nevada, California. *Geology*, **21**, 331–334.

Ruina, A. L. 1983. Slip instability and state variable friction laws. *J. Geophys. Res.* **88**, 10359–10370.

Rutter, E. H. 1976. The kinematics of rock deformation by pressure solution. *Phil. Trans. R. Soc.* **A283**, 203–219.

Rutter, E. H. 1986. On the nomenclature of mode of failure transitions in rocks. *Tectonophys.* **122**, 381–387.

Scholz, C. H. 1988. The brittle–plastic transition and the depth of seismic faulting. *Geol. Rund.* **77**, 319–328.

Shand, S. J. 1916. The pseudotachylyte of Parijs (Orange Free State) and its relation to trap-shotten gneiss and flinty crush-rock. *Q.J. Geol. Soc. Lond.* **72**, 198–221.

Shimamoto, T. 1986. Transition between frictional slip and ductile flow for halite shear zones at room temperature. *Science* **231**, 711–714.

Shimamoto, T. 1989. The origin of S–C mylonites and a new fault zone model. *J. Struct. Geol.* **11**, 51–64.

Sibson, R. H. 1975. Generation of pseudotachylite by ancient seismic faulting. *Geophys. J. R. Astron. Soc.* **43**, 775–794.

Sibson, R. H. 1977. Fault rocks and fault mechanisms. *J. Geol. Soc. Lond.* **133**, 191–213.

Sibson, R. H. 1980. Transient discontinuities in ductile shear zones. *J. Struct. Geol.* **2**, 165–171.

Sibson, R. H. 1984. Roughness at the base of the seismogenic zone: contributing factors, *J. Geophys. Res.* **89**, 5791–5799.

Spray, J. G. 1987. Artificial generation of pseudotachylite using friction welding apparatus: simulation of melting on a fault plane. *J. Struct. Geol.* **9**, 49–60.

Spray, J. G. 1992. A physical basis for the frictional melting of some rock-forming minerals. In: *Frictional Melting Processes and Products in Geological Materials, Tectonophys.* (edited by Magloughlin, J. F. & Spray, J. G.). **204**, 205–221.

Stern, T. W., Bateman, P. C., Morgan, B. A., Newell, M. F. & Peck, D. L. 1981. *Isotopic U–Pb Ages of Zircon from the Granitoids of the Central Sierra Nevada, California.* U.S. Geological Survey Professional Paper 1185, 17p.

Stesky, R. 1978. Mechanisms of high temperature frictional sliding in Westerly granite. *Can. J. Earth Sci.* **15**, 361–375.

Strehlau, J. 1986. A discussion of the depth extent of rupture in large continental earthquakes. In: *Earthquake Source Mechanics.* (edited by Das, S., Boatwright, J. & Scholz, C.). *AGU Geophys. Mono.* **37**, 131–146.

Swanson, M. T. 1988. Pseudotachylite-bearing strike-slip duplex structures in the Fort Foster Brittle Zone, S. Maine. *J. Struct. Geol.* **10**, 813–828.

Swanson, M. T. 1992. Fault structure, wear mechanisms and rupture processes in pseudotachylyte generation. In: *Frictional Melting Processes and Products in Geological Materials, Tectonophys.* (edited by Magloughlin, J. F. & Spray, J. G.). **204**, 223–242.

Tobisch, O. T., Saleeby, J. B., Renne, P. R., McNulty, B. A. & Tong, W. 1995. Variations in deformation fields during development of a large volume magmatic arc, central Sierra Nevada, California. *Geol. Soc. Am. Bull.* **107**, 148–166.

Toyoshima, T. 1990. Pseudotachylyte from the main zone of the Hidaka Metamorphic belt, Hokkaido, Japan. *J. Meta. Geol.* 507–523.

Tse, S. T. & Rice, J. R. 1986. Crustal earthquake instability in relation to the depth variation of frictional slip properties. *J. Geophys. Res.* **91**, 9452–9472.

Tullis, J. A. & Yund, R. A. 1985. Dynamic recrystallization of feldspar: a mechanism for ductile shear zone formation. *Geology*, **13**, 238–241.

Tullis, J. A. & Yund, R. A. 1987. Transition from cataclastic flow to dislocation creep of feldspar: mechanisms and microstructures. *Geology*, **15**, 606–609.

Wenk, H. R. 1978. Are pseudotachylites products of fracture or fusion? *Geology*, **6**, 507–511.

Wenk, H. R. & Weiss, L. E. 1982. Al-rich calcic pyroxene in pseudotachylyte: an indicator of high pressure and temperature. *Tectonophys.* **84**, 329–341.

White, S. H. 1976. The effects of strain on the microstructures, fabrics, and deformation mechanisms in quartzites. *Phil. Trans. R. Soc. Lond.* **A283**, 69–86.

Wong, I. G. & Chapman, D. S. 1990. Deep intraplate earthquakes in the western United States and their relationship to lithospheric temperatures. *Bull. Seismol. Soc. Am.* **80**, 589–599.

Wong, I. G. & Savage, W. U. 1983. Deep intraplate seismicity in the western Sierra Nevada, central California. *Bull. Seismol. Soc. Am.* **73**, 797–812.